Electronic Supplementary Material (ESI) for Journal of Materials Chemistry C.

Supporting Information

Optimization, selective and efficient production of CNTs/$Co_xFe_{3-x}O_4$ core/shell nanocomposites as outstanding microwave absorbers

Mei Wu,[a] Abdou Karim Darboe,[a] Xiaosi Qi [a,b,c,1*] Ren Xie,[a] Shuijie Qin,[a] Chaoyong Deng,[b] Guanglei Wu,[d] Wei Zhong,[c,*]

[a]*College of Physics, Guizhou Province Key Laboratory for Photoelectrics Technology and Application, Guizhou University, Guiyang City 550025, People's Republic of China*

[b]*Key Laboratory of Electronic Composites of Guizhou Province, Guizhou University, Guiyang City 550025, People's Republic of China*

[c]*National Laboratory of Solid State Microstructures and Jiangsu Provincial Laboratory for NanoTechnology, Nanjing University, Nanjing 210093, People's Republic of China*

[d]*Institute of Materials for Energy and Environment, State Key Laboratory of Bio-fibers and Eco-textiles, College of Materials Science and Engineering, Qingdao University, Qingdao 266071, P. R. China;*

*Corresponding author. Phone: +86-25-83621200. Fax: +86-25-83595535

E-mail: xsqi@gzu.edu.cn, wzhong@nju.edu.cn

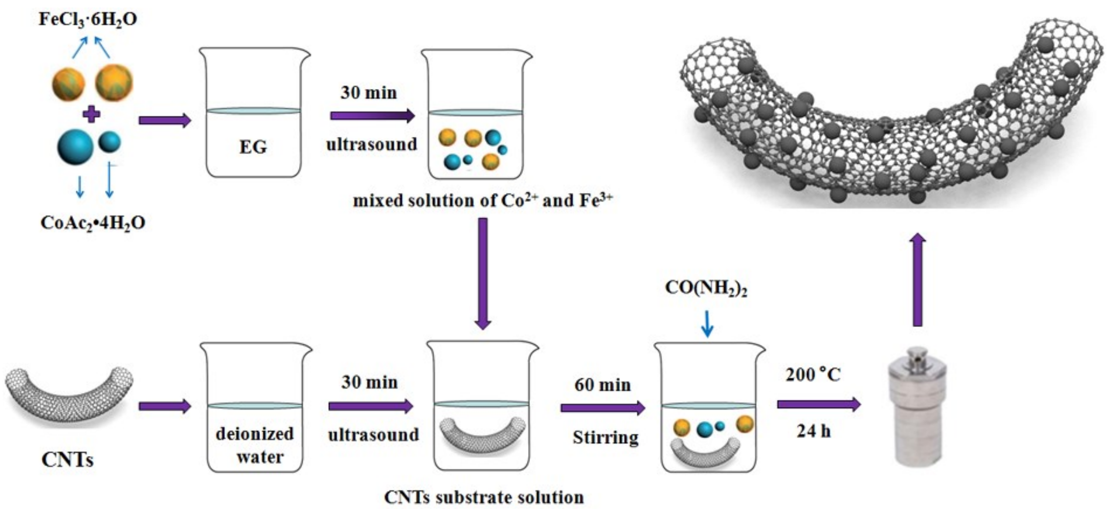

Figure S1. Schematic scheme for the synthesis process of CNTs-based NCs-I.

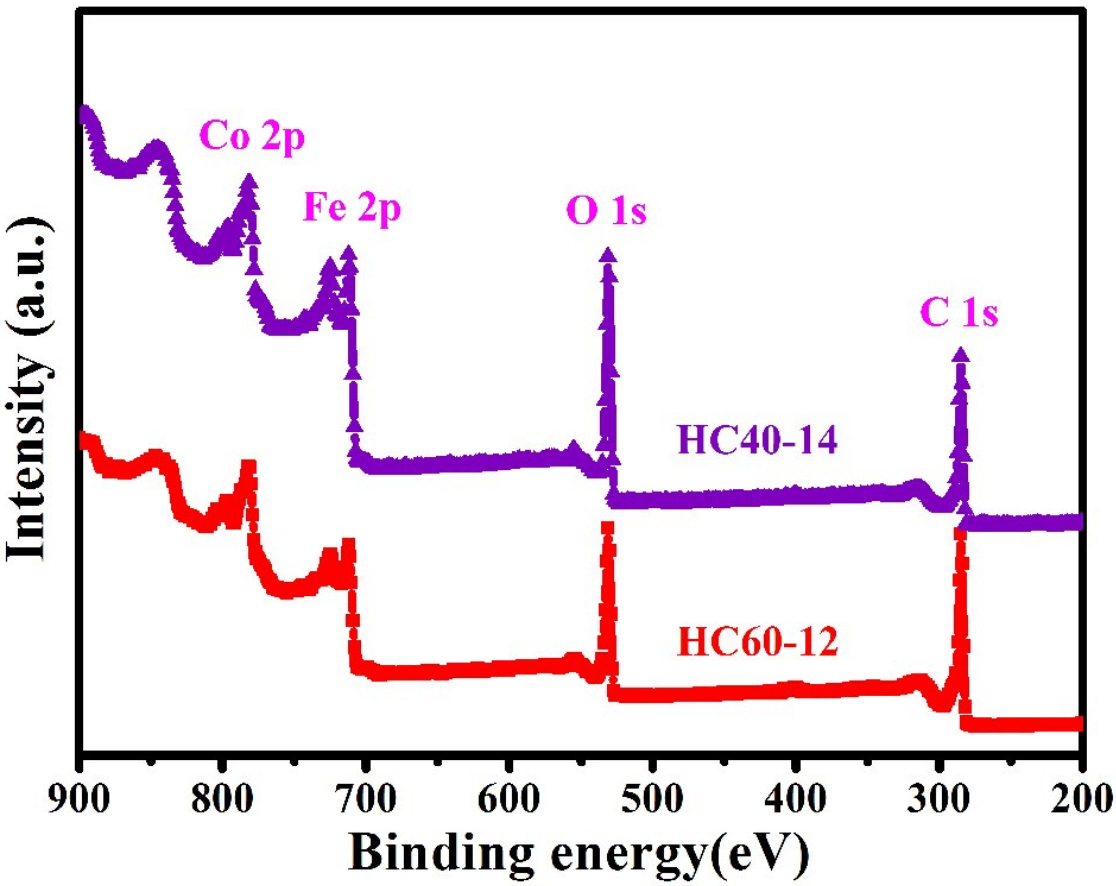

Figure S2. XPS spectra of the obtained HC40-14 and HC60-12.

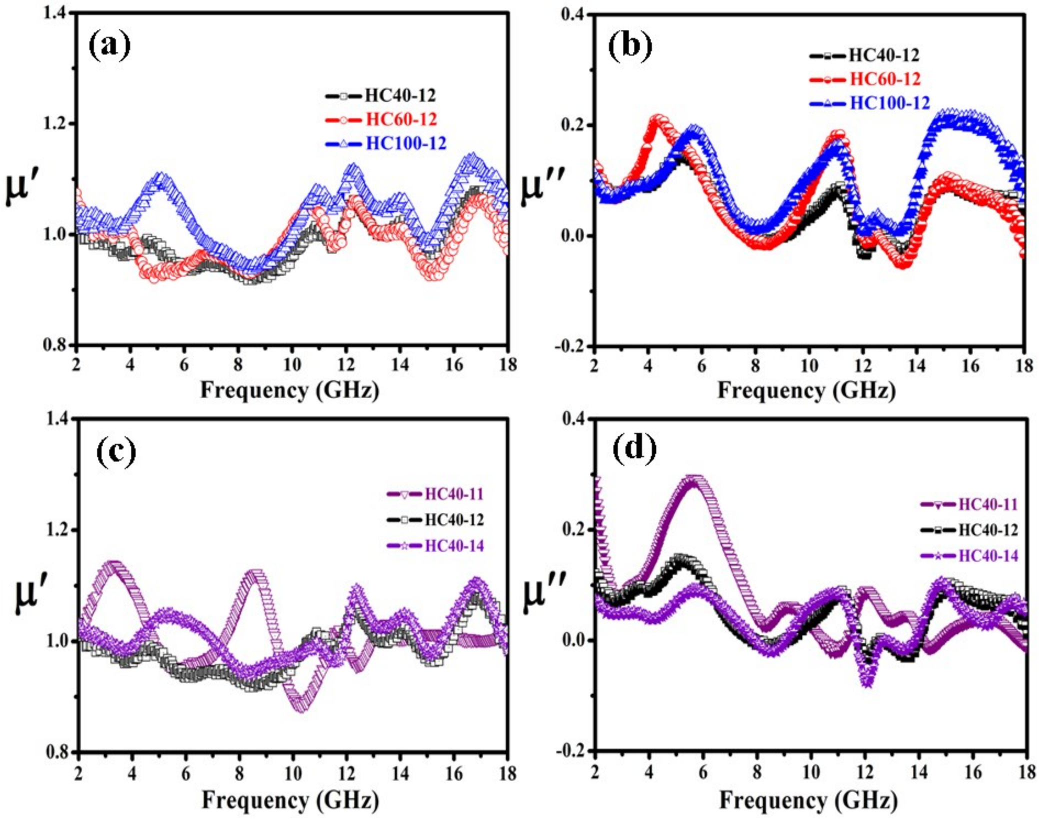

Figure S3. (a) Real part, and (b) imaginary part of complex permeability for the as-prepared samples, respectively.

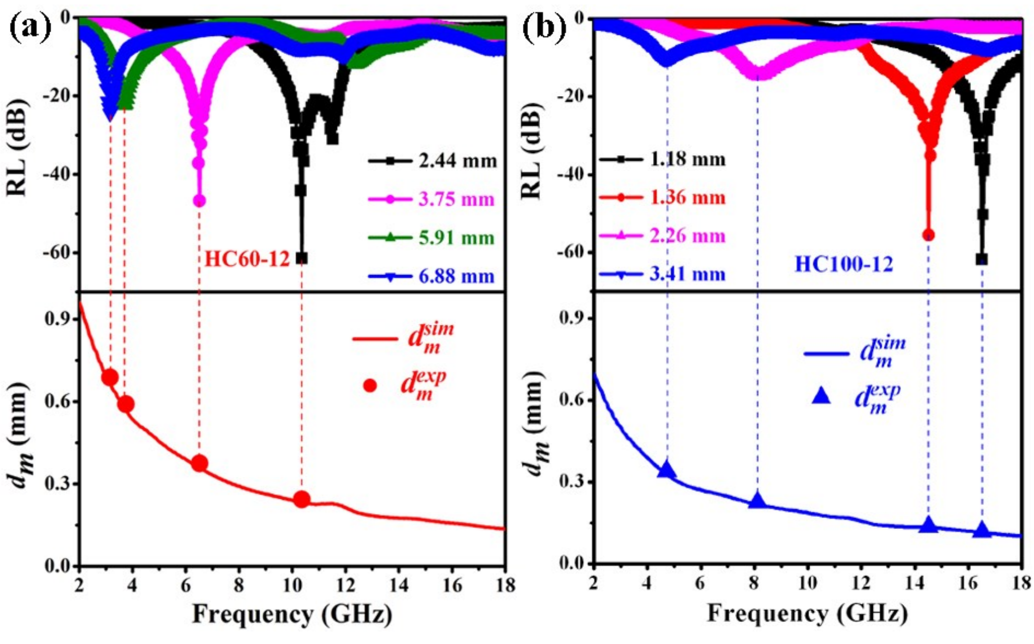

Figure S4. Comparison results between the experimental d_m values and theoretical curves for HC60-12 and HC100-12.

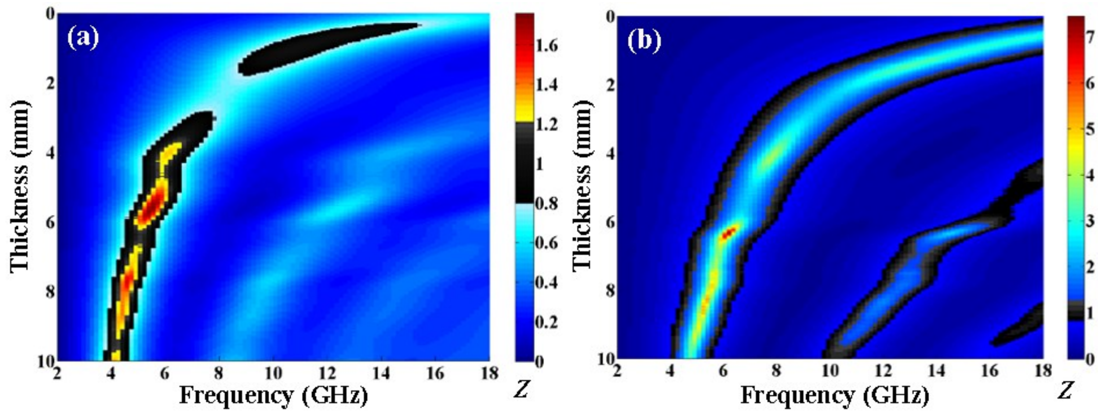

Figure S5. Impedance matching characteristics of (a) HC40-11, and (b) HC40-14.

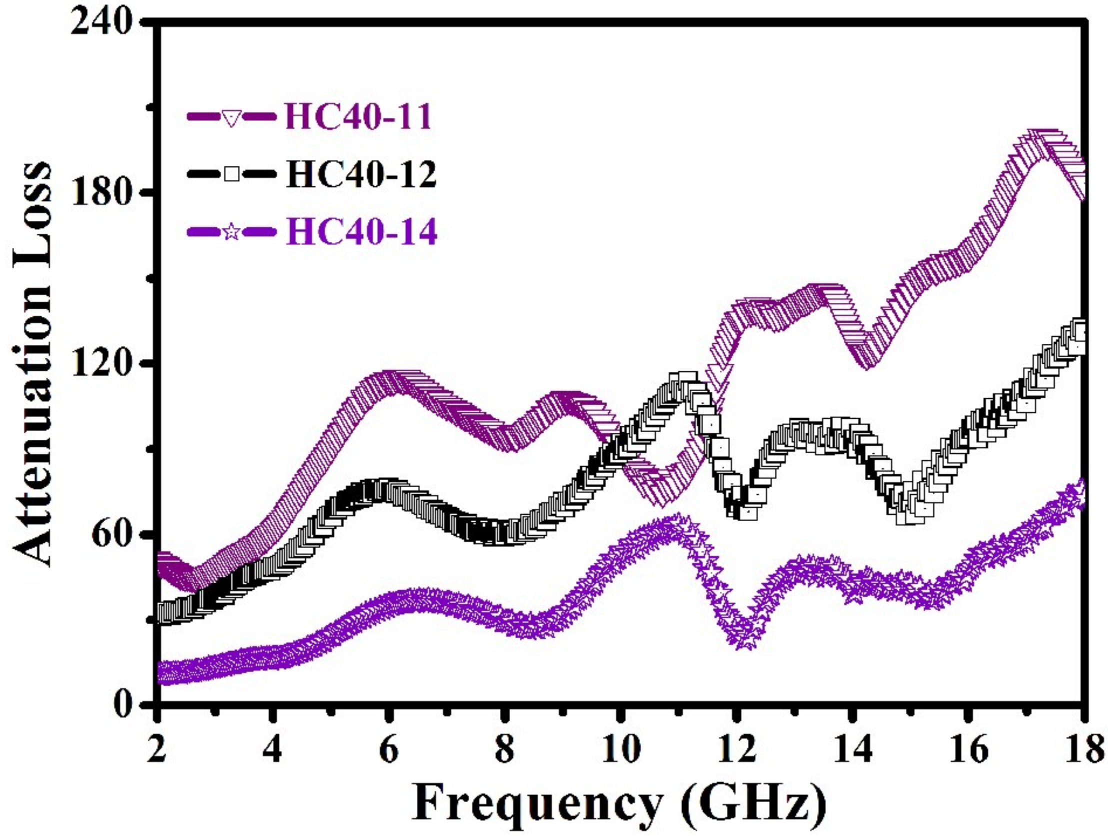

Figure S6. Frequency-dependent attenuation constant curves for the as-prepared HC40-11, HC40-12 and HC40-14 samples.

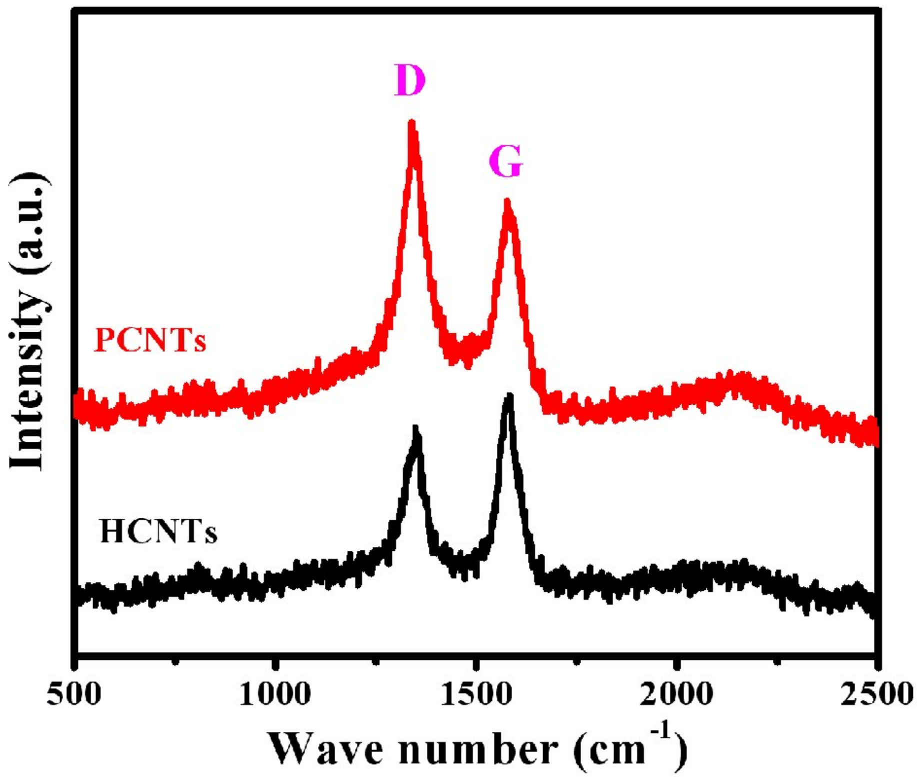

Figure S7. Raman spectra of HCNTs and PCNTs, respectively.

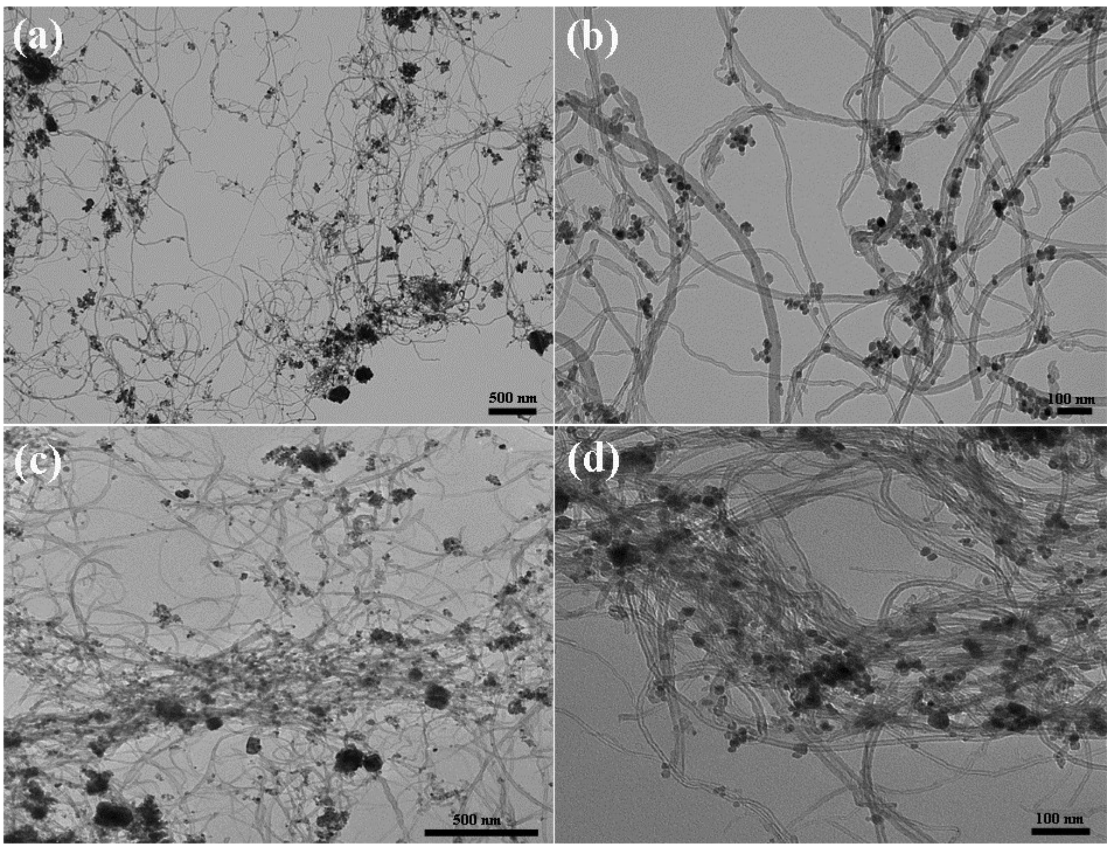

Figure S8. TEM images of (a,b) PC40-12, and (c,d) PC40-13, respectively.

Table S1. Summarized sheet for the effect of experimental parameters on the as-prepared core@shell structure CNTs-based NCs-I.

Experiments	Names of Sample	Composition	Effect on Microstructure
i	HC40-12	$CoCO_3$ and $Co_xFe_{3-x}O_4$	Number of nanoparticles decreases gradually with enhancing the amount of HCNTs
	HC60-12	$Co_xFe_{3-x}O_4$	
	HC100-12	$Co_xFe_{3-x}O_4$	
ii	HC40-11	$CoCO_3$ and $Co_xFe_{3-x}O_4$	Much more $Co_xFe_{3-x}O_4$ nanoparticles assemble together with decreasing the molar ratio of Co:Fe
	HC40-12	$CoCO_3$ and $Co_xFe_{3-x}O_4$	
	HC40-13	$Co_xFe_{3-x}O_4$	
	HC40-14	$Co_xFe_{3-x}O_4$	
iii	HC40-14	$Co_xFe_{3-x}O_4$	Number of nanoparticles decreases with increasing the amount of HCNTs
	HC60-14	$Co_xFe_{3-x}O_4$	
	HC80-14	$Co_xFe_{3-x}O_4$	
iv	PC40-12	$CoCO_3$ and $Co_xFe_{3-x}O_4$	Number of nanoparticles anchoring on the surface of PCNTs decreases evidently compared to HCNTs
	PC40-13	$Co_xFe_{3-x}O_4$	

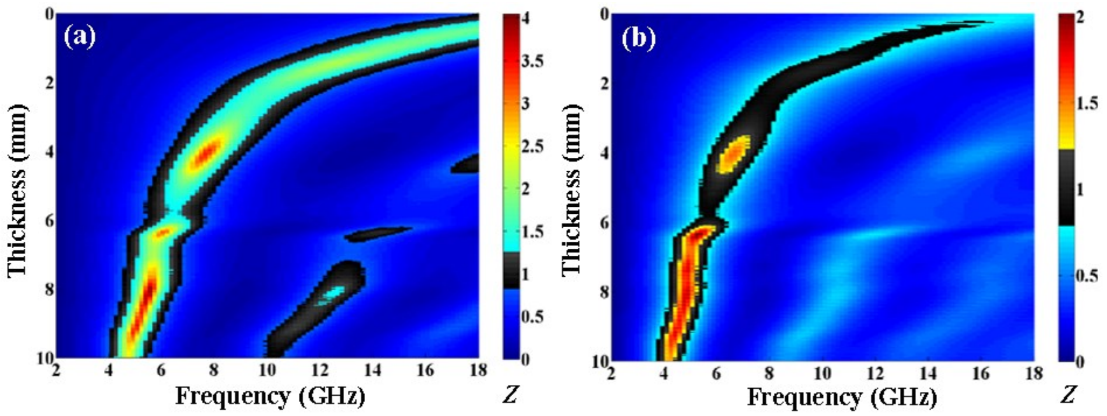

Figure S9. Impedance matching characteristics of (a) HC60-14, and (b) HC80-14.

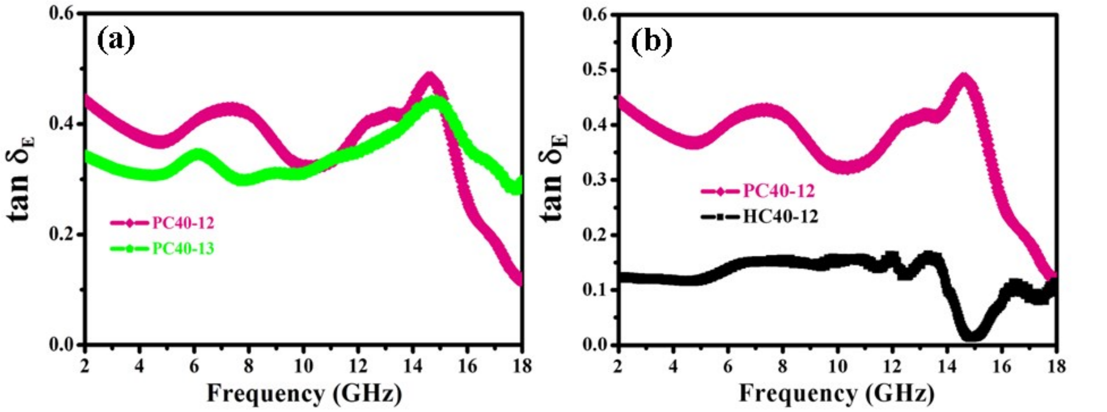

Figure S10. Dielectric loss tangent values of (a) PC40-12 and PC40-13, and (b) PC40-12 and HC40-12, respectively.

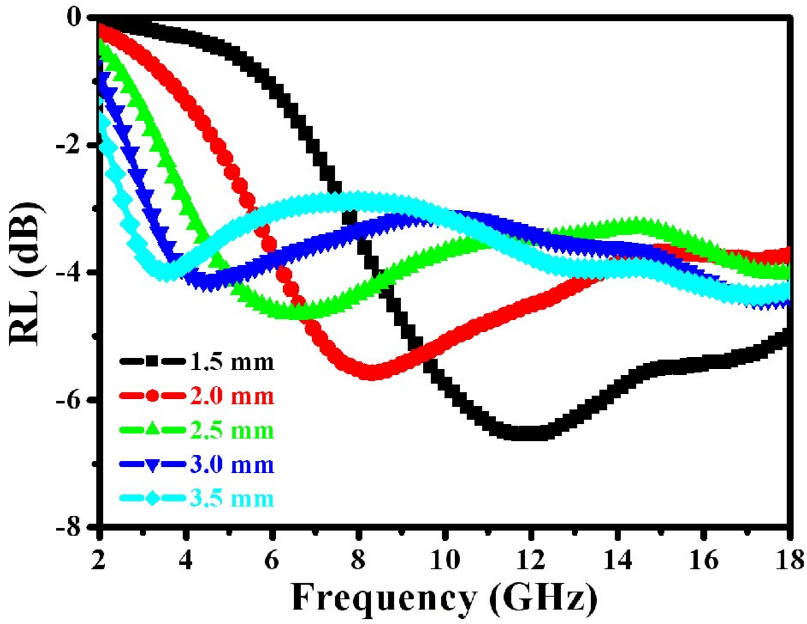

Figure S11. Microwave absorption characteristic curves of PCNTs.

Table S2. Summarized comprehensive EMWAPs of the as-prepared core@shell structure CNTs-based NCs-I.

Names of Sample	RL_{min} (dB)	d_m (mm)	AB_{max} (GHz)	d_m (mm)
HC40-12	-58.82	9.31	2.88	3.05
HC60-12	-61.4	2.44	3.64	2.76
HC100-12	-61.86	1.18	4.08	1.35
HC40-11	-49.96	3.18	4.40	1.64
HC40-12	-58.82	9.31	2.88	3.05
HC40-14	-47.28	10	1.72	9.01
HC60-14	-56.2	7.52	2.72	6.89
HC80-14	-62	3.46	3.20	2.75
PC40-12	-63.32	2.43	4.28	1.58
PC40-13	-67.18	4.63	4.52	1.76
PCNTs	-7.32	1.12	-	-

Table S3. Comparison results of comprehensive EMWAPs for the as-prepared core@shell structure CNTs-based NCs-I with the recently reported representative magnetic particles modified CNTs.

Names of Sample	RL_{min} (dB)	d_m (mm)	AB_{max} (GHz)	d_m (mm)	References
HC100-12	-61.86	1.18	4.08	1.35	This work
HC40-11	-49.96	3.18	4.40	1.64	This work
PC40-12	-63.32	2.43	4.28	1.58	This work
PC40-13	-67.18	4.63	4.52	1.76	This work
3D Fe_3O_4/CNTs	-59.2	1.68	3.1	1.68	S1
$ZnFe_2O_4$@CNT	-54.5	2.4	2.2	2.5	S2
CNTs/$Co_{0.5}Zn_{0.5}Fe_2O_4$	-64.7	3.1	4.3	2.1	S3
CeO_2-CNT	-40.95	3.5	1.8	3.5	S4
CNTs/$NiCo_2O_4$	-45.1	2.5	4.4	1.5	S5
FeCo-C-CNTs	-79.2	2	6.3	2	S6
CNTs/$ZnFe_2O_4$	-55.5	1.5	3.6	1.5	S7
3D Fe_3O_4-CNTs	-52.8	6.8	2.2	6	S8
Fe_3O_4-CNTs-HPCFs	-50.9	2.5	5.8	2.5	S9
Co-C/CNTs	-50	2.4	4.3	1.8	S10
$Li_{0.3}Zn_{0.3}Co_{0.1}Fe_{2.3}O_4$@CNT	-21	1	4.4	2	S11
Fe_3O_4@CNTs	-39.27	2	2.9	2	S12

References

S1. X.J. Zeng, L.Y. Zhu, B. Yang, R.H. Yu, *Mater. Design*, 2020,**189**, 108517.

S2. F. Li, W.W. Zhan, Y.T. Su, S. H. Siyal, Gang. Bai, W. Xiao, A.S. Zhou, Gang Sui, X.P. Yang, *Compos. Part A*, 2020, **133**, 105866.

S3. R.W. Shu , Y. Wu, Z.Y. Li , J.B. Zhang, Z.L. Wan, Y. Liu, M.D. Zheng, *Compos. Sci.Technol.*, 2019, **184**, 107839.

S4. Z.Q. Wang, P.F. Zhao, P.W. Li, S.D. Li, L.S. Liao, Y.Y. Luo, Z. Peng, D.N. He, Y. Cheng, *Compos. Part B*, 2019, **167**, 477-486.

S5.Q.M. Hu, R.L. Yang, Z.C. Mo, D.W. Lu, L.L. Yang, Z.F. He, H. Zhu, Z.K. Tang, X.C. Gui, *Carbon*, 2019, **153**, 737-744.

S6. D.T. Kuang, L.Z. Hou, S.L. Wang, H. Luo, L.W. Deng, J.L. Mead, H. Huang, M. Song, *Carbon*, 2019, **153**, 52-61.

S7. R.W. Shu, G.Y. Zhang, X. Wang, X. Gao, M. Wang, Y. Gan, J.J. Shi, J. He, *Chem. Eng. J.*, 2017, **337**, 242-255.

S8. Y.H. Chen, Z.H. Huang, M.M. Lu, W.Q. Cao, J. Yuan, D.Q. Zhang, M.S. Cao, *J. Mater. Chem. A*, 2015, **3**, 12621-12625.

S9. J. Qiu, T.T. Qiu, *Carbon*, 2015, 81, 20 -28.

S10. R.W. Shu, W.J. Li, Y. Wu, J.B. Zhang, G.Y. Zhang, *Chem. Eng. J.*, 2019, **362**, 513-524.

S11. M. Dalal, J.M. Greneche, B. Satpati, T.B. Ghzaiel, F. Mazaleyrat, R.S.Ningthoujam, P.K. Chakrabarti, *ACS Appl. Mater. Interfaces*, 2017, **9**, 40831-40845.

S12. S.Y. Liu, L.F. Mei, X.L. Liang, L.B. Liao, G.C. Lv, S.F. Ma, S.Y. Lu, A. Abdelkader, K. Xi, ACS Appl. Mater. Interfaces, 2018, **10**, 29467-29475.